E-ISSN 2586-9027
Homepage : https://tci-thaijo.org/index.php/SciTechAsia
Science & Technology Asia
Vol. 31 No.3 July - September 2026
Page: [173-186]
Original research article

Valorization of Geothermal Silica Waste in the Fabrication of PVA-Based Nanofiber via Electrospinning: Morphological, Mechanical, and Surface Property Evaluation

Kusno Isnugroho[1,*], Yusup Hendronursito[1], Tumpal O Rajagukguk[2], Rama Khadafi[2]

[1]*Research Center for Mineral Technology, Research Organization for Nanotechnology and Materials, National Research and Innovation Agency, Lampung 35361, Indonesia*
[2]*Department of Mechanical Engineering, Faculty of Engineering, Malahayati University, Bandar Lampung 35152, Indonesia*

Received 18 October 2025; Received in revised form 29 July 2026
Accepted 3 August 2026; Available online 30 September 2026

ABSTRACT

This study explores the valorization of geothermal silica waste as a functional filler for the fabrication of polyvinyl alcohol (PVA)-based nanofibers via electrospinning. Geothermal silica was processed through a sol–gel route and incorporated at varying weight fractions (0–7 wt%) into PVA solutions before electrospinning. The resulting nanofiber mats were characterized in terms of morphology, elemental composition, chemical structure, mechanical properties, and surface wettability using FESEM-EDS, FTIR, Vickers hardness testing, and water contact angle measurements. Silica incorporation influenced the nanofiber morphology, reducing the average fiber diameter to 170 nm at 5 wt% silica loading; however, excessive silica content promoted bead formation and fiber fusion due to limited silica dispersion within the PVA matrix. EDS and FTIR analyses confirmed the incorporation of geothermal-derived silica within the PVA nanofiber matrix. Mechanical evaluation revealed that 1 wt% silica loading exhibited the highest hardness value (20.36 HV), while higher silica concentrations reduced mechanical performance due to morphological defects and silica aggregation. Surface wettability analysis showed improved hydrophilic behavior with increasing silica loading up to 5 wt%, while excessive silica addition resulted in reduced wettability due to morphological heterogeneity. These findings demonstrate that geothermal silica waste can be successfully converted into functional PVA/silica nanofibers composites, highlighting the importance of silica loading optimization to achieve balanced mechanical and surface properties for potential membrane-related applications and circular economy strategies.

***Corresponding author:** kusn010@brin.go.id
doi.org/10.70730/sta.v31i3.268395

Keywords: Electrospinning; Geothermal; Morphological properties; Nanofiber ; PVA; Waste

1. Introduction

Nanofiber-based materials have attracted considerable attention in materials engineering due to their high specific surface area, porosity, structural flexibility, and ease of surface functionalization [1-3]. These properties enable applications in filtration, sensing, separation, biomedical treatments, and energy systems [4-8]. Among various fabrication methods, electrospinning is widely used for its simplicity and precise control over fiber morphology [9]. The process employs a high-voltage electric field to draw polymer solutions or melts into continuous nanofibers, forming nonwoven mats [10]. Polyvinyl alcohol (PVA) is often used owing to its water solubility, chemical stability, biocompatibility, and excellent spinnability [11], though its limited mechanical strength and thermal stability require reinforcement with fillers. Silica (SiO_2) has been incorporated into PVA nanofibers to improve mechanical, thermal, and surface properties [12-14]. Commonly, silica is synthesized through sol–gel processes using precursors such as tetraethyl orthosilicate (TEOS) [15]. Furthermore, silica surfaces can be chemically modified using silane coupling agents or antimicrobial agents, such as 3-chloropropyltrimethoxysilane (CPTS) and benzalkonium chloride (BAC), to introduce specific functionalities including improved interfacial compatibility or antibacterial properties [16]. Other studies have integrated cellulose nanofibers from rice husk—naturally rich in silica—into PVA to enhance crystallinity and thermal stability [17]. Combining sol–gel synthesis with electrospinning can yield PVA/silica nanofibers with antibacterial properties [16], and silica–carbon quantum dot hybrids in PVA have shown high bioactivity for medical uses [18].

Research on waste-derived silica, such as from volcanic ash, has mostly targeted composite membranes or adsorbents via phase inversion or casting, with limited use in direct electrospinning integration [19]. Electrospun silica-based nanofibers still rely heavily on commercial precursors like sodium silicate or TEOS, which require chemical processing to produce nanoscale silica suitable for polymer matrices. Additional surface functionalization is often employed to enhance compatibility and impart specific properties. Pure silica nanofibers from TEOS typically involve sol–gel processing and calcination to achieve high purity [20].

However, TEOS-based approaches generally require additional chemical precursors and processing steps, which may reduce the sustainability advantage compared with waste-derived silica sources [21, 22]. Rice husk–derived silica offers a natural alternative but often requires energy-intensive processing and shows limitations in advanced applications [23]. In contrast, geothermal waste, a by-product of geothermal power operations, contains abundant amorphous silica with high surface area and reactivity, typically >90% SiO_2 with minor Al_2O_3, Fe_2O_3, and CaO impurities [24-26]. The amorphous structure promotes better adhesion within polymer matrices, improving interfacial bonding in PVA–silica composites. Using geothermal silica offers processing advantages over rice husk silica, as it avoids high-temperature combustion and harsh leaching, aligning with green chemistry and circular economy principles. Valorizing geothermal by-products into functional materials reduces waste and dependence on synthetic chemicals, while achieving mechanical and thermal properties comparable to those from synthetic silica sources.

This study proposes the direct incorporation of geothermal waste–derived silica into PVA nanofibers via a sol–gel route followed by electrospinning. The approach addresses two main gaps: the underutilization of industrial silica waste streams in high-value nanofiber applications, and the lack of research integrating waste-derived silica directly into

electrospun structures rather than post-processing or using membrane casting methods. The work also aims to establish structure–property relationships for varying silica loadings, providing insight into optimal filler content for balancing fiber uniformity, mechanical performance, and functional attributes. By replacing conventional synthetic precursors with geothermal silica, the method supports sustainable manufacturing while expanding the application potential of electrospun nanofibers in fields such as filtration, adsorption, and functional membranes for environmental and biomedical purposes.

2. Materials and Methods

The experimental procedure was adapted from previous studies [15, 25, 27], with modification involving the replacement of conventional silica sources with geothermal waste-derived silica. This modification aims to utilize geothermal waste as an alternative silica precursor and supports waste valorization strategies aligned with circular economy principles.

2.1 Materials

Polyvinyl alcohol (PVA, Mw~85,000–124,000, 98–99% hydrolyzed) was purchased from Sigma-Aldrich. Geothermal sludge was collected from the silica deposition area of the Geothermal Power Plant in Ulu Belu, Lampung Province, Indonesia. The collected sludge was subsequently dried and processed to obtain geothermal-derived silica precursor. Nitric acid (HNO_3, 65%), ethanol (C_2H_5OH, analytical grade), and deionized water were used throughout the process. All chemicals were of analytical grade and used without further purification.

2.2 Preparation of Silica from geothermal sludge

Geothermal sludge was initially dried at 105°C for 24 h, followed by grinding and sieving to obtain particles below 200 µm. The silica precursor was extracted through an acid-assisted sol–gel process. Briefly, 10 g of dried geothermal sludge was mixed with 100 mL of 2 M HNO_3 and stirred at 70°C for 2 h. The mixture was filtered, and the obtained filtrate was adjusted to pH 7 using NH_4OH to induce silica gel formation. The gel was aged for 24 h, dried at 100°C, and calcined at 600°C for 3 h to improve silica purity and obtain a stable silica powder. The chemical composition of the obtained silica powder was analyzed using XRF to determine its SiO_2 content.

2.3 Fabrication of PVA/Silica nanofibers via electrospinning

The overall fabrication procedure of PVA/silica nanofiber membranes via electrospinning is illustrated schematically in Fig. 1. The process consists of PVA solution preparation, silica sol preparation, homogenization of the spinning solution, electrospinning fabrication, and subsequent characterization.

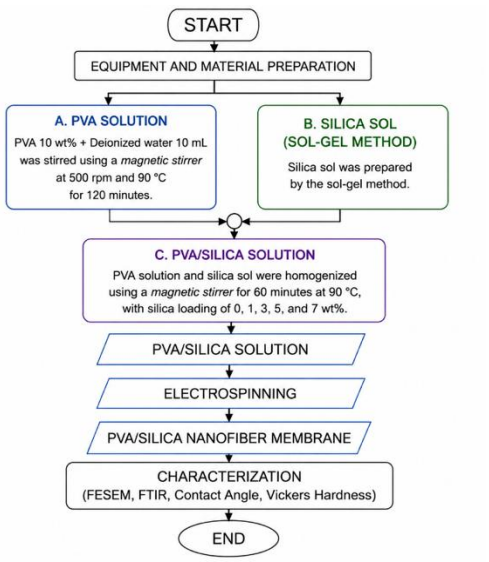


Fig. 1. Schematic representation of the fabrication process of geothermal silica-based PVA nanofiber membranes via electrospinning.

A 10 wt% PVA solution was prepared by dissolving PVA in deionized water under magnetic stirring at 90 °C for 2 h until a homogeneous solution was obtained. The solution was then cooled to room temperature

before silica incorporation. Geothermal-derived silica-rich powder was added at different concentrations (0, 1, 3, 5, and 7 wt% relative to PVA content) and ultrasonicated for 30 min to improve silica dispersion within the polymer solution.

The prepared spinning solution was transferred into a syringe equipped with a stainless-steel needle (0.6 mm inner diameter). Electrospinning was conducted under an applied voltage of 20 kV, a flow rate of 0.5 mL h^{-1}, and a tip-to-collector distance of 15 cm. The generated nanofibers were collected on aluminum foil and dried at room temperature for 24 h to remove residual moisture.

The obtained nanofiber samples were coded according to silica loading as follows: NFS0 (0 wt% silica), NFS1 (1 wt% silica), NFS3 (3 wt% silica), NFS5 (5 wt% silica), and NFS7 (7 wt% silica).

2.4 Characterization

The morphology and elemental composition of the nanofiber membranes were analyzed using field emission scanning electron microscopy coupled with energy dispersive spectroscopy (FESEM-EDS) (Thermo Scientific Quattro S). Fourier transform infrared spectroscopy (FTIR) (Bruker Invenio-R) was employed to identify the characteristic functional groups and chemical interactions within the nanofiber membranes. Although tensile testing is commonly used for fibrous membranes, Vickers hardness was selected in this study as a comparative indicator of local surface mechanical resistance and structural rigidity of the nanofiber mats. Vickers hardness measurements were performed using a Zwick Roell microhardness tester with an applied load of 100 g and a dwell time of 10 s to evaluate the mechanical response of the nanofiber membranes. Water contact angle measurements were conducted using a DSA25E goniometer to evaluate the surface wettability characteristics.

The properties of pristine PVA nanofibers and PVA nanofibers incorporating geothermal-derived silica were compared. The evaluated parameters included average fiber diameter, Si elemental distribution, chemical bonding characteristics, hardness, and water contact angle.

3. Results and Discussion

3.1 Chemical composition of geothermal-derived Silica

The chemical composition of geothermal-derived silica powder was analyzed using XRF, as summarized in Table 1. The result revealed that SiO_2 was the dominant component with a concentration of 94.743 wt%, indicating the effectiveness of the extraction process in producing a silica-rich material from geothermal sludge.

Table 1. Chemical composition of geothermal-derived silica powder obtained from XRF analysis.

Oxide	Content (wt%)
SiO_2	94.743
Fe_2O_3	2.623
CaO	0.795
P_2O_5	0.660
K_2O	0.503
MgO	0.337
TiO_2	0.184
Others	<0.2

Trace/ minor oxide components, including Fe_2O_3 (2.623 wt%), CaO (0.795 wt%), K_2O (0.503 wt%), and P_2O_5 (0.660 wt%), were also detected. The presence of these minor oxides is associated with residual mineral constituents originating from geothermal deposits and rock–fluid interactions during geothermal processes. Nevertheless, the high SiO_2 concentration indicates that the obtained material can be considered a silica-rich precursor suitable for incorporation into the PVA nanofiber matrix.

Further confirmation of silica incorporation within the nanofiber matrix was subsequently evaluated through FTIR and EDS analyses.

3.2 Morphological analysis of PVA/Silica nanofibers

The morphology of PVA/silica nanofiber membranes with different silica loadings was investigated using FESEM and fiber diameter distribution analysis, as presented in Figs. 2–6. The FESEM images revealed progressive changes in fiber morphology with increasing silica loading, including variations in fiber diameter, surface uniformity, and defect formation. In the NFS0 sample (Fig. 2), the nanofibers exhibited an average diameter of 228 ± 40.6 nm with a relatively wide diameter distribution. The nanofiber network showed relatively uniform morphology; however, several isolated beads were still observed. Pure PVA solutions generally produce fine fibers; nevertheless, defects such as bead formation may occur due to the competition between electrostatic forces, solution viscosity, and surface tension during the electrospinning process [18].

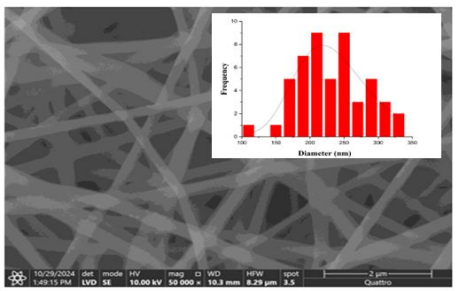


Fig. 2. FESEM image, and diameter distribution of sample NFS0.

In the NFS1 sample (Fig. 3), the average fiber diameter slightly increased to 250 ± 54.7 nm compared with pristine PVA (NFS0), accompanied by a narrower diameter distribution. This variation suggests that low silica loading does not necessarily result in diameter reduction, as fiber morphology is influenced by the combined effects of solution viscosity, conductivity, and polymer–filler interactions during electrospinning. The FESEM image showed a relatively uniform and nearly bead-free fiber network. This observation is consistent with previous findings reporting that small amounts of inorganic fillers can improve electrospinning jet stability by modifying solution conductivity and polymer–filler interactions, resulting in more uniform fiber formation [28].

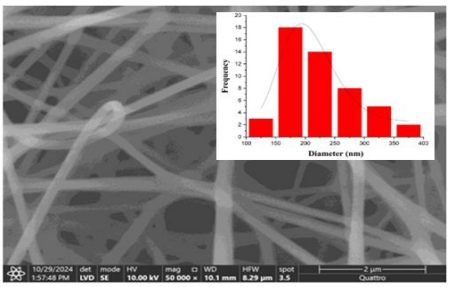


Fig. 3. FESEM image, and diameter distribution of sample NFS1.

In the NFS3 sample (Fig. 4), the average fiber diameter decreased to 208 ± 49.6 nm compared with NFS0 and NFS1, accompanied by a narrower diameter distribution mainly within the range of 100–250 nm. The reduction in fiber diameter suggests that moderate silica incorporation influenced the electrical and rheological characteristics of the PVA solution, promoting more efficient jet stretching during electrospinning. However, FESEM images revealed the initial appearance of small bead-like structures, indicating slight instability in the electrospinning process. This behavior may be related to changes in solution properties and silica dispersion within the PVA matrix, which affect jet stability during fiber formation [27].

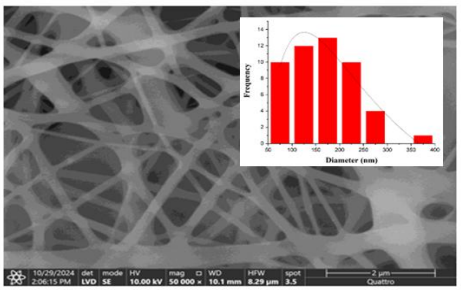


Fig. 4. FESEM image, and diameter distribution of sample NFS3.

In the NFS5 sample (Fig. 5), the fibers exhibited the smallest average diameter of 170

± 56.8 nm; however, the broader diameter distribution indicates increased morphological heterogeneity due to the coexistence of ultrafine and thicker fibers. The FESEM image revealed the formation of large beads, fiber fusion, and non-uniform fiber morphology.

These observations suggest that higher silica loading may induce silica aggregation, which disrupts fiber continuity and promotes morphological defects [29]. Although NFS5 exhibited the smallest average fiber diameter, the increased diameter variation indicates that the reduction in fiber size was accompanied by deterioration of morphological uniformity.

Therefore, excessive silica incorporation may contribute to continued jet stretching and diameter reduction while simultaneously causing silica aggregation and fiber fusion, which negatively affect the structural integrity of the nanofiber network.

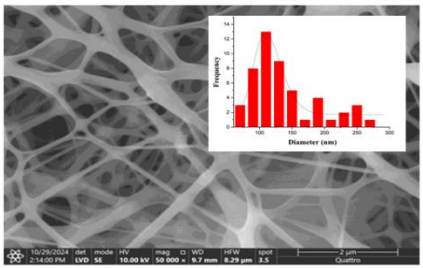


Fig. 5. FESEM image, and diameter distribution of sample NFS5.

In the NFS7 sample (Fig. 6), the average fiber diameter increased again to 225 ± 43.2 nm, accompanied by a relatively broad diameter distribution. This increase suggests that excessive silica loading altered the electrospinning behavior by affecting solution properties and fiber formation dynamics. The FESEM image showed relatively continuous fiber structures; however, fiber fusion between adjacent fibers remained evident. The observed morphology is consistent with previous studies, which reported that increasing inorganic filler content can modify fiber formation behavior and improve fiber network compactness within an optimum loading range, while excessive filler addition may induce structural defects [30].

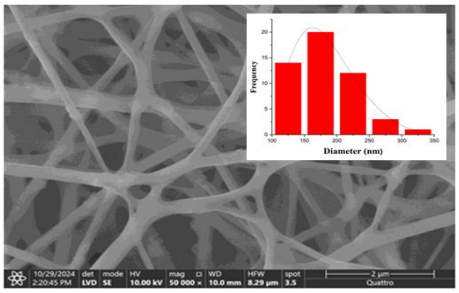


Fig. 6. FESEM image, and diameter distribution of sample NFS7.

Overall, the results indicate that relatively favorable morphological characteristics were obtained at low to moderate silica loadings (1–3 wt%), where improved silica dispersion, controlled fiber diameter, and reduced defect formation were observed. At higher silica loadings, silica aggregation and fiber fusion became more pronounced, resulting in increased morphological heterogeneity. This observation agrees with composite reinforcement principles, where non-uniform filler dispersion can act as structural defects and reduce the effectiveness of stress transfer within the polymer matrix.

3.3 Hardness analysis of PVA/Silica nanofibers

The Vickers hardness results of PVA/silica nanofibers membranes with different silica loadings are presented in Fig. 7.

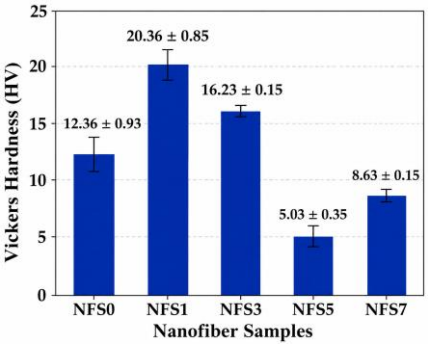


Fig. 7. Average Vickers hardness of PVA/Silica nanofibers.

The average hardness values exhibited clear variations depending on the silica content. For NFS0, the hardness value was recorded at 12.36 ± 0.93 HV. In NFS1, the hardness increased to 20.36 ± 0.85 HV, indicating a strengthening effect associated with improved silica dispersion and enhanced interaction between silica particles and the PVA matrix. This improvement can be attributed to the incorporation of silica-derived fillers, which restrict polymer chain mobility, enhance interfacial stress transfer, and contribute to increased stiffness of the nanocomposite network.

The physical interactions between silica-derived fillers and the PVA matrix facilitate stress transfer and restrict polymer chain mobility, contributing to improved mechanical reinforcement [31]. In the NFS3 sample, the hardness value decreased to 16.23 ± 0.15 HV; however, it remained higher than pristine PVA (NFS0), indicating that silica incorporation still contributed to mechanical enhancement. This reduction may be associated with changes in solution properties and silica dispersion behavior, which can influence jet stability, fiber formation, and stress transfer efficiency within the nanofiber network. Similar observations were reported by Pirzada et al. [21], who demonstrated that variations in silica/PVA ratios can modify solution properties and subsequently affect fiber morphology and mechanical performance. Excessive filler loading may reduce reinforcement efficiency due to particle aggregation and non-uniform stress distribution within the polymer matrix.

This trend was evident in the NFS5 sample, where the hardness decreased sharply to 5.03 ± 0.35 HV. FESEM analysis revealed substantial silica aggregation, bead formation, and fiber fusion, which can act as stress concentration sites within the nanofiber structure and reduce stress transfer efficiency. EDS analysis further confirmed the presence of silica within the PVA matrix. For NFS7, the hardness increased slightly to 8.63 ± 0.15 HV but remained significantly lower than the optimum value observed for NFS1. This modest recovery may be associated with improved fiber continuity compared with NFS5; however, silica aggregation and structural defects were still present at high silica loading.

The relationship between average fiber diameter and Vickers hardness of the PVA/silica nanofiber membranes is presented in Fig. 8. The correlation was evaluated by plotting fiber diameter as the independent variable and hardness value as the dependent variable. The linear fitting indicates the general relationship between these two parameters; however, the correlation demonstrates that fiber diameter alone is insufficient to determine the mechanical response of the nanofiber membranes. Although the NFS5 sample exhibited the smallest average fiber diameter (170 nm), it showed the lowest hardness value (5.03 HV), which was attributed to silica aggregation, fiber fusion, and increased morphological defects. Therefore, the mechanical performance of PVA/silica nanofibers is governed not only by fiber diameter but also by silica dispersion, polymer–filler interfacial interaction, and structural integrity of the nanofiber network.

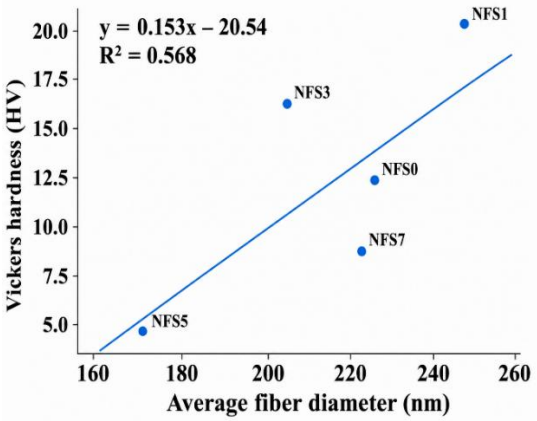


Fig. 8. Relationship between average fiber diameter and Vickers hardness of PVA/silica nanofiber membranes with different silica contents.

Although a reduction in fiber diameter is generally expected to improve fiber uniformity and potentially enhance mechanical performance, the NFS5 sample exhibited an opposite behavior. NFS5 possessed the smallest average fiber diameter (170 ± 56.8 nm) but showed the lowest hardness value (5.03 ± 0.35 HV). This result indicates that fiber diameter alone is insufficient to determine the mechanical performance of the nanofiber membrane. Other structural factors, particularly fiber morphology, silica dispersion, and defect formation, significantly influenced the mechanical response. In the NFS5 sample, the presence of silica aggregation, bead formation, and fiber fusion generated structural discontinuities that reduced stress transfer efficiency and weakened the nanofiber network. The lower hardness of NFS5 is attributed to excessive silica incorporation, which may promote silica aggregation and affect electrospinning jet stability. These effects can generate morphological defects such as bead formation and fiber fusion, resulting in reduced structural uniformity and inefficient stress transfer within the nanofiber network. Therefore, the mechanical reinforcement effect of silica depends not only on fiber diameter reduction but also on effective filler dispersion, interfacial interaction between silica and PVA, and preservation of the fibrous structure.

3.4 Elemental composition analysis by EDS

The elemental composition and spatial distribution of elements within the PVA/silica nanofiber membranes were investigated using energy dispersive spectroscopy coupled with field emission scanning electron microscopy (FESEM-EDS). Figure 9 presents the FESEM images and elemental mapping results of selected samples (NFS0, NFS3, and NFS7), representing the pristine PVA membrane, intermediate silica loading, and highest silica loading, respectively. The EDS mapping provides information regarding the spatial distribution of C, O, Si, and minor inorganic elements within the nanofiber membrane structure.

The FESEM images of the selected samples reveal interconnected fibrous networks within the nanofiber membranes. The elemental mapping results show the presence of C and O elements, which are mainly associated with the PVA polymer matrix. The relatively uniform distribution of C and O elements is consistent with the homogeneous distribution of the PVA component throughout the nanofiber structure, confirming the formation of a continuous polymer-rich phase.

In the NFS0 sample, the FESEM image reveals a continuous fibrous network without the presence of silica-related elements. The EDS mapping shows only C and O as dominant elements, corresponding to the chemical composition of the PVA matrix. The uniform distribution of these elements confirms the homogeneous polymer phase in the pristine PVA nanofiber membrane.

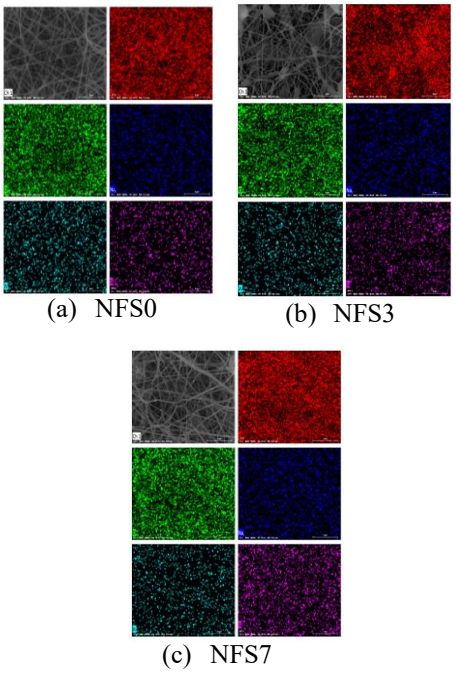


Fig. 9. FESEM images and corresponding EDS elemental maps of (a) NFS0, (b) NFS3, and (c) NFS7 PVA/silica nanofiber membranes.

In addition to C and O, Si signals were detected in silica-containing nanofiber samples, confirming the presence of geothermal-derived silica within the PVA matrix. The Si distribution became more evident with increasing silica loading, suggesting a higher contribution of silica-derived components within the nanofiber structure. The detection of Si is consistent with the XRF composition of the silica precursor and supports the FTIR identification of silica-related bonding characteristics within the nanofiber matrix.

The EDS analysis also detected minor amounts of Na and Al elements, which may originate from residual mineral components associated with geothermal silica waste. These minor elements reflect the natural mineral composition of the geothermal-derived silica source. However, their relatively low signals compared with Si indicate that silica-derived components remain the predominant inorganic species detected within the nanofiber structure.

Semi-quantitative EDS analysis revealed that the detected Si content increased from 0.16 wt% in NFS0 to 0.66 wt% in NFS3 and further increased to 1.60 wt% in NFS7. The small Si signal detected in NFS0 is likely associated with background contribution, substrate effects, or instrumental detection limitations. Although slight variations were observed among samples, these differences can be attributed to the localized nature of EDS analysis and the heterogeneous morphology of electrospun nanofiber membranes.

3.5 Contact angle analysis of PVA/Silica nanofibers

The contact angle measurements presented in Fig. 10, for samples NFS0, NFS1, NFS3, NFS5, and NFS7 demonstrate the effect of increasing silica content on the surface wettability of the nanofiber membranes. The contact angle values for each sample were measured with water droplets as the test liquid at 20°C.

The analysis is as follows: the initial sample without silica (NFS0, Fig. 10a) exhibited an average contact angle of 43.7°. This relatively low value indicates a hydrophilic surface, which is typical for pure PVA due to the presence of abundant hydroxyl (–OH) groups capable of forming hydrogen bonds with water molecules. This strong hydrophilic behavior facilitates the spreading of water on the surface, consistent with previous studies reporting contact angles between 40° and 50° for electrospun PVA membranes [32-34].

Upon the addition of 1 wt% (NFS1, Fig. 10b) silica, the contact angle slightly decreased to an average of 41.3° (41.9° left, 40.7° right). This reduction suggests an enhancement in hydrophilicity, attributed to the introduction of silanol (Si–OH) groups on the silica nanoparticle surface, which are highly polar and capable of hydrogen bonding with water. Moreover, the homogeneous dispersion of silica nanoparticles likely increased the effective polar surface area [35].

In NFS3 (Fig. 10c), the contact angle further decreased to 34.9°, indicating a significant improvement in wettability. This result implies that at moderate silica loading, the polar groups are well-distributed, and the surface roughness induced by nanoparticles enhances the spreading of water. The synergistic effect of PVA's hydroxyl groups and silica's silanol groups optimizes surface hydrophilicity at this composition [35]. For NFS5 (Fig. 10d), the contact angle decreased even more to 29.8° (30.7° left, 28.9° right), representing the highest hydrophilicity among all samples. This may be due to the optimal balance between silica dispersion and the creation of micro/nano-scale roughness, leading to improved water spreading according to the Wenzel wetting model. However, at this stage, excessive silica loading may begin to risk agglomeration if further increased [36]. Interestingly, the NFS7 (Fig. 10e) sample exhibited an increase in contact angle to an average of 42.75° (45.8° left, 39.7° right), indicating a reduction in hydrophilicity compared to NFS5. This behavior is likely caused by nanoparticle agglomeration at

higher loadings, which reduces the number of accessible hydrophilic groups on the membrane surface. Such agglomerates may create localized hydrophobic regions, decreasing the overall wettability [37].

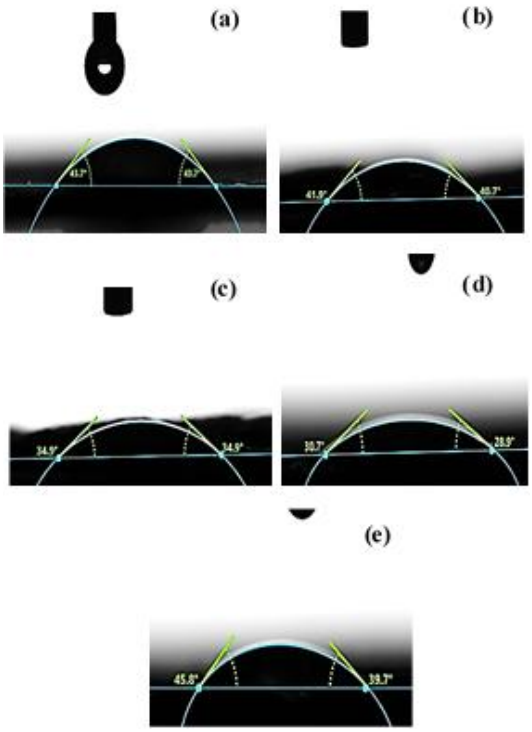


Fig. 10. Contact angle measurements of nanofiber membranes: (a) NFS0, (b) NFS1, (c) NFS3, (d) NFS5, and (e) NFS7, using water droplets at 20 °C.

The decrease in water contact angle from 43.7° for NFS0 to 29.8° for NFS5 indicates enhanced surface wettability due to the hydrophilic nature of silica and the presence of surface hydroxyl groups. However, further silica addition (NFS7) increased the contact angle, which may be associated with silica agglomeration and heterogeneous surface morphology that reduced the accessibility of hydrophilic sites.

3.6 FTIR spectroscopy

The FTIR spectrum of the PVA/silica nanofibers (NFS0-NFS7) in Fig. 11, shows the presence of the main functional groups of the PVA matrix and silica filler from the sol-gel synthesis. FTIR spectra of PVA/silica nanofibers with varying silica content.

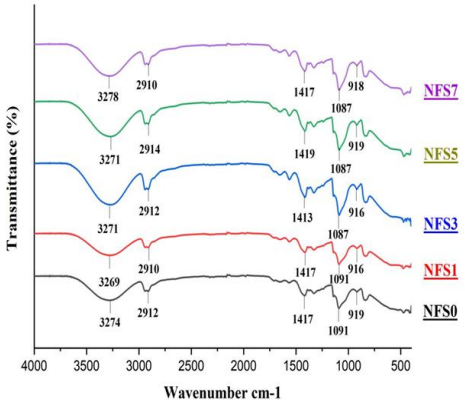


Fig. 11. FTIR spectra of PVA/silica nanofibers with different silica loadings (NFS0–NFS7).

The broad peaks at 3270-3278 cm-¹ were identified as stretching O-H hydroxyl groups derived from PVA and silanol (Si-OH) groups on silica particles [38]. Variation in the O–H band intensity may be associated with the overlapping contributions of hydroxyl groups from PVA and silica-derived silanol groups. The band at 2910-2914 cm-¹ is related to the C-H stretching of the -CH_2 group in the PVA backbone. The position and intensity of this band is relatively constant across all samples, indicating that the main structure of PVA remains intact despite the addition of silica [39].

The band at 1413–1419 cm^{-1} originates from C–H bending vibrations, while the absorption band at 1087–1091 cm^{-1} is attributed to Si–O–Si asymmetric stretching vibrations, which are characteristic of silica network structures [40–41]. The appearance of Si–O–Si related bands in silica-containing samples indicates the presence of silica-derived structures within the PVA matrix and supports the incorporation of geothermal-derived silica during nanofiber fabrication. In addition, the band at 916–919 cm^{-1} can be associated with Si–OH related vibrations originating from incompletely condensed silanol groups. The presence of these silanol groups provides potential sites for hydrogen

bonding interactions between PVA chains and silica surfaces, which may contribute to improved interfacial adhesion between the polymer matrix and silica particles [42].

This observation is consistent with the Vickers hardness results, where the 1 wt% silica composition (NFS1) exhibited the highest hardness value (20.36 HV). This improvement may be associated with better silica dispersion and enhanced interfacial interactions between the PVA matrix and silica particles, which facilitate stress transfer within the nanofiber network. In contrast, at higher silica loading (≥5 wt%), the mechanical performance decreased, which can be attributed to morphological changes observed from FESEM analysis, including silica aggregation and fiber fusion. These structural defects may act as stress concentration sites and reduce the efficiency of stress transfer within the nanofiber network. From a surface property perspective, the presence of silanol (Si–OH) and hydroxyl (O–H) groups may contribute to enhanced hydrophilic behavior of the nanofiber surface. This behavior is reflected in the contact angle measurements, where silica-containing samples generally exhibited lower contact angles due to improved interaction between hydrophilic surface groups and water molecules.

Overall, FTIR analysis supports the incorporation of geothermal-derived silica into the PVA nanofiber matrix through the identification of silica-related vibrations and hydroxyl groups. These chemical characteristics provide insight into the possible interactions between PVA and silica, which may contribute to the observed changes in mechanical performance and surface wettability of the nanofiber membranes.

4. Conclusion

This study successfully produced PVA-based nanofibers reinforced with geothermal silica synthesized via the sol–gel method and fabricated through electrospinning. Morphological analysis revealed that silica incorporation at low to medium concentrations (1–3 wt%) improved fiber uniformity and reduced morphological defects. The highest hardness value (20.36 HV) was achieved with 1 wt% silica, whereas the optimal balance between mechanical properties and surface wettability was obtained at 3 wt% silica, exhibiting a hardness value of 16.23 HV and a water contact angle of 34.9°. FTIR analysis confirmed the presence of silica-related bonds, including Si–O–Si and Si–OH groups, which contributed to the modification of surface characteristics.

The novelty of this research lies in the direct utilization of geothermal silica waste, processed via the sol–gel method without additional functionalization, as a low-cost and environmentally friendly filler for nanofiber production. The results demonstrate the potential of this material for membrane and filtration applications requiring a balance between mechanical strength and improved hydrophilicity, while providing a sustainable approach for converting geothermal waste into value-added materials.

The relationship between surface wettability and mechanical performance demonstrated that silica incorporation influenced different functional properties of PVA nanofiber membranes. Although increased silica loading improved hydrophilic behavior due to silica-associated hydroxyl groups, excessive silica addition resulted in morphological defects that reduced mechanical performance. Among the investigated compositions, NFS3 provided the most balanced combination of surface wettability (34.9° contact angle) and mechanical properties (16.23 HV hardness), supported by relatively uniform nanofiber morphology. These findings indicate that controlling silica loading is essential for optimizing the multifunctional performance of PVA/silica nanofiber membranes.

Future studies should investigate the reproducibility of high silica-loading formulations through repeated electrospinning experiments using independent batches of geothermal silica precursor. Additional

quantitative analysis of silica dispersion and interfacial interactions may also provide deeper understanding of the reinforcement mechanism.

Acknowledgements

The authors gratefully acknowledge the facilities and technical support provided by the Advanced Characterization Laboratories Lampung, National Research and Innovation Agency (BRIN), through the E-Layanan Sains platform.

References

[1] Chen J, Yu Z, Li C, Lv Y, Hong S, Hu P, Liu Y. Review of the principles, devices, parameters, and applications for centrifugal electrospinning. Macromol Mater Eng. 2022;307:2200057.

[2] Kenry, Lim CT. Nanofiber technology: Current status and emerging developments. Prog Polym Sci. 2017;70:1–17.

[3] Zhang F, Si Y, Yu J, Ding B. Electrospun porous engineered nanofiber materials: A versatile medium for energy and environmental applications. Chem Eng J. 2023;456:140989.

[4] Lyu C, Zhao P, Xie J, Dong S, Liu J, Rao C, et al. Electrospinning of nanofibrous membrane and its applications in air filtration: A review. Nanomaterials. 2021;11:1501.

[5] Kim G, Doh SJ, Kim Y, Oh HJ, Lee GD, Im JN. Electrospun polyvinyl alcohol composite nonwovens for air filtration materials in the humidity environment. Fibers Polym. 2022;23:690–8.

[6] Mai Z, Liu Q, Bian Y, Wang P, Fu X, Lin D, et al. PCL/collagen/UA composite biomedical dressing with ordered microfiberous structure fabricated by a 3D near-field electrospinning process. Polymers. 2022;15:223.

[7] Thielke MW, Guzmán SL, Tafoya JP, Tamayo EG, Castro C, Hosseinaei O, et al. Full lignin-derived electrospun carbon materials as electrodes for supercapacitors. Front Mater. 2022;9:859872.

[8] Wang B, Wang J, Lou Y, Ding S, Xu J, Liu F, et al. Halloysite nanotubes strengthened electrospinning composite nanofiber membrane for on-skin flexible pressure sensor. Appl Clay Sci. 2022;228:106650.

[9] Song J, Lin X, Ee LY, et al. A review on electrospinning as versatile supports for diverse nanofibers and their applications in environmental sensing. Adv Fiber Mater. 2023;5:429–60.

[10] Liu Q, Luo S, Peng J, Chang R. Electrospun nanofibers from plant natural products: A new approach toward efficient wound healing. Int J Nanomedicine. 2024;19:13973–90.

[11] Zhu M, Han J, Wang F, Shao W, Xiong R, Zhang Q, et al. Electrospun nanofibers membranes for effective air filtration. Macromol Mater Eng. 2017;302:1600353.

[12] Bhardwaj N, Kundu SC. Electrospinning: A fascinating fiber fabrication technique. Biotechnol Adv. 2010;28:325–47.

[13] Sabra O, Hussein A, Obaid M. Preparation and evaluation of water resistance, mechanical and morphological characteristics of PVA/SiO_2 nanocomposites for food industry applications. Dig J Nanomater Biostruct. 2021;16:733–45.

[14] Chen Y, Fan H, Zha X, et al. Fabrication of silica/PVA-co-PE nanofiber membrane for oil/water separation. Fashion Text. 2021;8:14.

[15] Kulczyńska J, Chibrikov V, Pawcenis D, Jędrzejczyk RJ, Sebastian V, Cybulska J, et al. Sustainable poly(vinyl alcohol)/chitosan electrospun nanofibers and casted films with bioactive additives. Ind Crops Prod. 2025;233:121335.

[16] Nirwan M, Setyawan H, Widiyastuti W. Synthesis of PVA/SiO_2 nanofibers by

electrospinning method for supercapacitor separators. IPTEK J Proc Ser. 2021;6:336.

[17] Rifansyah TBI. Pengaruh variasi SiO_2 dalam nanofiber PVA/SiO_2 dari silika sekam padi menggunakan metode electrospinning. Skripsi, Universitas Lampung; 2022 (unpublished).

[18] Bjorge D, Daels N, De Vrieze S, Dejans P, Van Camp T, Audenaert W, et al. Performance assessment of electrospun nanofibers for filter applications. Sep Purif Technol. 2011;81:231–8.

[19] Gharibi A, Kashefi M, Nasrollahzadeh M. Recent advances in the electrospinning of polymer nanofibers and their applications in water treatment. RSC Adv. 2019;9:17436–55.

[20] Zhafira N, Kurniawan F, Aziz M. Utilization of volcanic ash waste as a raw material for silica synthesis in composite membrane fabrication. J Environ Chem Eng. 2023;11:110783.

[21] Syahrul S, Putri DA, Hartati H. Zeolite-based composite membranes for heavy metal removal from aqueous solutions: A review. Mater Today Proc. 2022;63:101–7.

[22] Zhang L, Zhang W, Yu D, Shen H. The preparation of electrospun PVA/silica nanofibers and their application in filtration. J Appl Polym Sci. 2021;138:50893.

[23] Wang H, Ding X, Li B. Preparation and characterization of electrospun poly(vinyl alcohol)/silica nanofiber membranes for water purification. J Membr Sci. 2020;596:117698.

[24] Ramakrishna S, Fujihara K, Teo WE, Lim TC, Ma Z. An introduction to electrospinning and nanofibers. Singapore: World Scientific; 2005.

[25] Pant B, Park M, Park SJ, Kim HY. Electrospun poly(vinyl alcohol) hybrid nanofibers containing functionalized silica nanoparticles for antibacterial applications. Colloids Surf A. 2019;572:66–72.

[26] Zhang X, Reagan MR, Kaplan DL. Electrospun silk biomaterial scaffolds for regenerative medicine. Adv Drug Deliv Rev. 2009;61:988–1006.

[27] Li D, Xia Y. Electrospinning of nanofibers: Reinventing the wheel? Adv Mater. 2004;16:1151–70.

[28] Huang ZM, Zhang YZ, Kotaki M, Ramakrishna S. A review on polymer nanofibers by electrospinning and their applications in nanocomposites. Compos Sci Technol. 2003;63:2223–53.

[29] Zong X, Kim K, Fang D, Ran S, Hsiao BS, Chu B. Structure and process relationship of electrospun bioabsorbable nanofiber membranes. Polymer. 2002;43:4403–12.

[30] Subbiah T, Bhat GS, Tock RW, Parameswaran S, Ramkumar SS. Electrospinning of nanofibers. J Appl Polym Sci. 2005;96:557–69.

[31] Agarwal S, Wendorff JH, Greiner A. Use of electrospinning technique for biomedical applications. Polymer. 2008;49:5603–21.

[32] Bhattarai N, Edmondson D, Veiseh O, Matsen FA, Zhang M. Electrospun chitosan-based nanofibers and their cellular compatibility. Biomaterials. 2005;26:6176–84.

[33] Doshi J, Reneker DH. Electrospinning process and applications of electrospun fibers. J Electrostat. 1995;35:151–60.

[34] Reneker DH, Chun I. Nanometre diameter fibres of polymer, produced by electrospinning. Nanotechnology. 1996;7:216–23.

[35] Greiner A, Wendorff JH. Electrospinning: A fascinating method for the preparation of ultrathin fibers. Angew Chem Int Ed. 2007;46:5670–703.

[36] Yang Q, Li Z, Hong Y, Zhao Y, Qiu S, Wang C, Wei Y. Influence of solvents on the formation of ultrathin uniform poly (vinyl pyrrolidone) nanofibers with

electrospinning process. Polymer. 2004;45:7151–64.

[37] Frenot A, Chronakis IS. Polymer nanofibers assembled by electrospinning. Curr Opin Colloid Interface Sci. 2003;8:64–75.

[38] Rahman Khan MM, Pal S, Hoque MM, Alam MR, Younus M, Kobayashi H. Simple fabrication of PVA-ZnS composite films with superior photocatalytic performance: Enhanced luminescence property, morphology, and thermal stability. ACS Omega. 2019;4:6144–53.

[39] Al-Emam E, Soenen H, Caen J, et al. Characterization of polyvinyl alcohol-borax/agarose (PVA-B/AG) double network hydrogel utilized for the cleaning of works of art. Herit Sci. 2020;8:106.

[40] Menazea AA, Ismail AM, Awwad NS, Ibrahium HA. Physical characterization and antibacterial activity of PVA/Chitosan matrix doped by selenium nanoparticles prepared via one-pot laser ablation route. J Mater Res Technol. 2020;9:9598–606.

[41] Salamah S, Mufandi I, Jumiati J, Fadhilah A. Synthesis and optimization of snake fruit peel ash-derived silica for iron (Fe) removal from batik wastewater. J Ilmu Lingkungan. 2025;23:54–61.

[42] Kesavan K, Agilan S, Muthukumarasamy N, Krishnasamy V, Vinitha G. Synthesis, characterization and nonlinear optical properties of Si/PVA-PEG nanocomposites. J Ovonic Res. 2020;16:355–60.